Developments in the nuclear magnetic resonance spectroscopy of lipids and membranes: the first quarter century

Eric Oldfield

Department of Chemistry, University of Illinois at Urbana-Champaign, 505 South Mathews Avenue, Urbana, IL 61801, U.S.A.

Introduction

In 1966, Chapman and Penkett [1] reported the first observation of high-resolution n.m.r. spectra of model membranes, and demonstrated in a convincing way the condensing effect of cholesterol on phospholipid acyl chains, at the molecular level. The lecithin/cholesterol system continues to be a paradigm for real biological membranes, such as the red cell and myelin, and over the past 25 years just about every new n.m.r. technique has been applied towards gaining an understanding of this complex system. In the following, we give a brief account of the progress in this area, right up until the present, where extremely highly resolved spectra of both model and biological membranes can now be obtained, which include some observations on membrane proteins themselves.

Developments in ^{1}H n.m.r. spectroscopy

We began our studies of lipids in membranes in 1968, using sonicated single-bilayer systems. However, there were always reservations about using sonication, especially for biomembranes, and thus new approaches had to be developed. One expansion of the very early ^{1}H n.m.r. experiments suggested by Chapman involved the use of the so-called 'magic-angle' sample spinning (MAS) method, in which lipids are spun rapidly (several kHz) in a gas turbine and the dipolar interactions between protons, which broaden static n.m.r. spectra, are averaged out as a result of sample rotation. Working with

Doskočilová and Schneider, we obtained modest resolution improvements [2], but the time was not yet right, as sensitivity and resolution at the low magnetic field strengths in use in 1972 (~ 1.4 Tesla) were simply inadequate for true high-resolution, although the results did look promising. Some 15 years later, we tried the same experiments again, this time using a high-field magnet (11.7 Tesla, 500 MHz for protons), together with the Fourier transform technique, and obtained very well resolved spectra, as shown in Fig. 1. The results we obtained were quite surprising in that the extremely broad 'super-Lorentzian' lineshapes observed by Lawson and Flautt [3] for smectic liquid crystals, which obscure high resolution features, broke up at even low spinning speeds into a manifold of sharp spinning sidebands [4], and truly high-resolution spectra were obtained [4, 5].

The observation of such high-resolution ^{1}H MAS n.m.r. spectra was surprising, since the static dipolar Hamiltonian:

$$\sum_{i<j} D_{ij}(\phi)(3I_{zi}I_{zj} - I_i \cdot I_j) \qquad (1)$$

does not in general commute with itself at different rotor orientations, ϕ. However, in most liquid crystalline phases, intermolecular dipole–dipole interactions are averaged by fast lateral diffusion, while fast axial rotation reduces the intramolecular dipole–dipole interaction and causes the angular dependence of the Hamiltonian to be the same for all proton pairs. Thus, the dipolar interaction is scaled by $P_2(\cos\theta)$, where θ is the angle between the director axis and H_0, such that

$$D_{ij} = \tfrac{1}{2}(3\cos^2\theta - 1)D^0_{ij} \qquad (2)$$

and the Hamiltonian becomes

$$\tfrac{1}{2}(3\cos^2\theta - 1)\sum_{i<j} D^0_{ij}(3I_{zi}I_{zj} - I_i \cdot I_j) \qquad (3)$$

which under MAS commutes with itself at different rotor orientations, ϕ. The result is that the dipole–dipole interaction becomes inhomogeneous and sharp spinning sidebands are obtained at sample rotation rates much slower than the static width. In addition, we also found that the envelope of the spinning sidebands in a slow-spin spectrum was very close to the theoretical 'super-Lorentzian' lineshape [3] given by [6]:

$$L(\upsilon - \upsilon_0) \propto \int_0^1 |3\cos^2\theta - 1|^{-1} \times f[(\upsilon - \upsilon_0)/|3\cos^2\theta - 1|]\, d\cos\theta \qquad (4)$$

Similar breakdown of the static lineshape into numerous sharp spinning sidebands has now been observed for most of the other smectic liquid crystalline phase lipids we have investigated, including monogalactosyldiglyceride, digalactosyldiglyceride, sulphoquinovosyldiglyceride, egg

Fig. 1. 500 MHz ^{1}H 'magic-angle' sample spinning n.m.r. spectrum of dimyristoylphosphatidylcholine/H_2O (50 wt.% ^2H_2O) at 30 °C

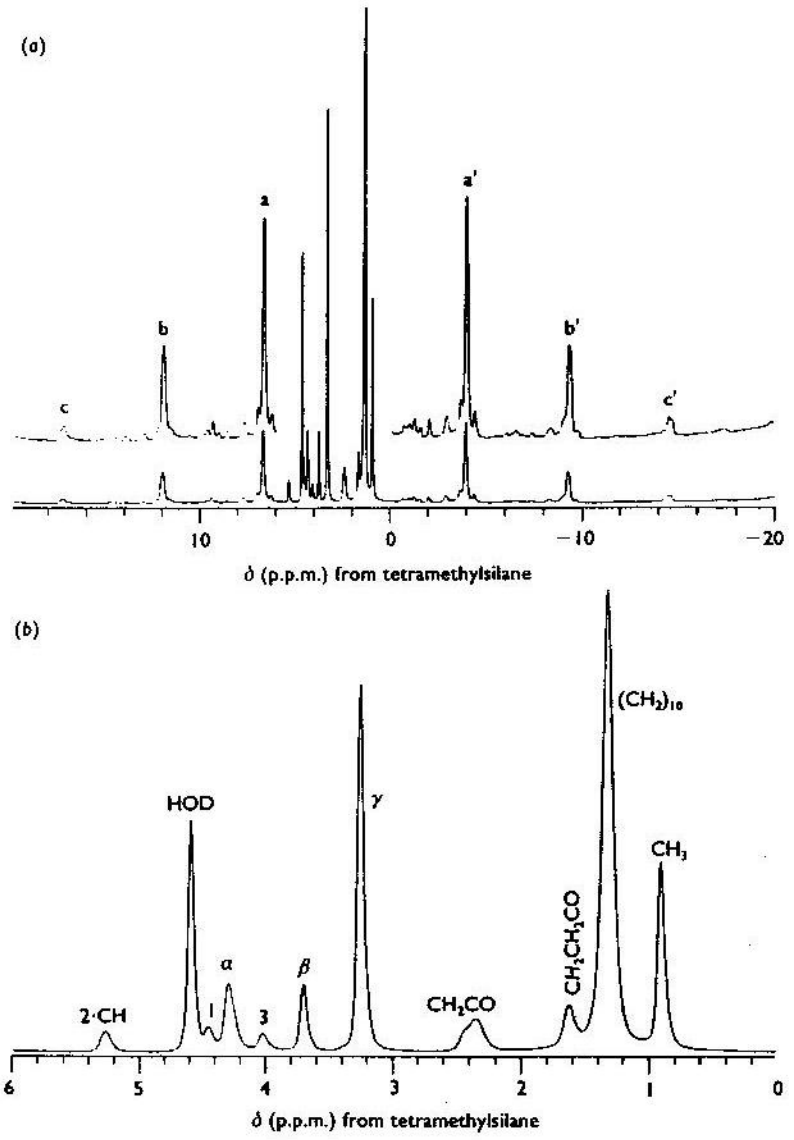

(a) Full spectrum; (b) centre-band region only. Reprinted from [5] with permission.

phosphatidylcholine, beef brain sphingomyelin, beef heart cardiolipin, potassium oleate-water, phosphatidylinositol, dioleoylphosphatidylcholine and dipalmitoylphosphatidylcholine.

We also found that molecular order parameters could, in some instances, be deduced from the side-band patterns [5], the results obtained agreeing strongly with those found using ^{2}H n.m.r. More recently, we have investigated the proton spin-lattice relaxation in lipid bilayers, but found only a rather small graduation in relaxation rates from one part of the lipid to another. This re-ignited the old controversy about the occurrence of spin-diffusion — the transfer of magnetization from one part of the lipid to another by means of energy-conserving mutual spin flip-flops, and the results of two dimensional n.m.r. experiments using isotopically ^{2}H-labelled molecules have tended towards a view that spin-diffusion does occur in these systems. This topic is now of particular interest in the area of contrast enhancement in magnetic resonance imaging (MRI).

Using MRI to study brain, it has been shown that white matter in myelin, which contains very large amounts of cholesterol, appears extremely 'bright' in relaxation-weighted MRI images, which means that the H_2O protons are relaxed much more effectively than in grey matter. These MRI images have been used to investigate brain development in infants, as well as the breakdown of myelin in e.g. multiple sclerosis and Koenig, Balabun and their colleagues [7, 8] have shown that cholesterol is likely to make a major contribution to the relaxation enhancement (or brightness). Looking at egg lecthin with and without cholesterol (the basic Chapman and Penkett system of 1966), these authors have found that water relaxation increases monotonically with cholesterol content and then flattens out at a ratio of 1:1 lecithin/cholesterol, as might be expected on the basis of known phase diagrams [9]. The results of other experiments have shown that the H_2O signal intensity can be altered by means of off-resonance irradiation of the lecithin/sterol protons, indicating cross-relaxation or spin-diffusion between H_2O and lipid, the large relaxation enhancement apparently being due to the presence of cholesterol (as demonstrated by use of a deuterated lipid plus cholesterol, where the same enhancement is seen). These experiments appear to fit in nicely with our own [4, 5] in which we have found that the cholesterol ring's protons are not visible in ^{1}H MAS experiments probably because of strong dipolar interactions in the cholesterol spin system, which is sufficient to bring about effective spin-diffusion.

In our laboratory, we have found that other interactions may also be important in H_2O relaxation. For example, as shown in Table 1, we find extremely rapid H_2O relaxation in the presence of the glycolipid digalactosyldiglyceride (DGDG), presumably because of strong interactions of H_2O with the sugar hydroxyl groups.

Because around one-third of the dry weight of myelin lipid consists of the glycosphingolipid, cerebroside, it seems likely that cerebroside galactosyl–water interactions could also play a role in contrast enhancement.

Table 1. Water proton spin-lattice relaxation times in lipid/water systems (K. D. Park & E. Oldfield, unpublished work)

System	T_1 H_2O (s)
Egg lecithin	2.2
Egg lecithin/cholesterol (1:1)	1.6
Digalactosyldiglyceride	1.1

Lipids are 1:1 wt ratio with H_2O.

Thus, the early work on lecithin/cholesterol dynamics and phase behaviour has gradually evolved, through studies of two-dimensional n.m.r. spin-diffusion and cross-relaxation, to the rapidly developing area of MRI contrast enhancement, where cholesterol has been shown to play a major role [7, 8] in differentiating grey from white matter, in both development and disease.

Applications of ^{2}H n.m.r. spectroscopy

The cholesterol story took a major turn in 1971 when, in collaboration with Chapman and Derbyshire (at Nottingham), we were able to show that ^{2}H n.m.r. spectroscopy of ^{2}H-labelled lipids was likely to be a rather useful technique for studying lipid (and later, protein) structure. Our initial studies involved the massive ^{2}H-labelling of the acyl side chains of 1,2-dimyristoyl-*sn*-glycero-3-phosphocholine (dimyristoylphosphatidylcholine, DMPC), and wide-line, continuous-wave n.m.r. [10], and we were pleased to see that gel phase, liquid-crystal phase and DMPC-cholesterol/water systems all had quite different spectra. The major quadrupole splitting (the 'plateau') of DMPC in the liquid-crystal phase was ~27 kHz, and this increased to ~50 kHz upon addition of an equimolar amount of cholesterol, which translates to about a factor of two increase in molecular order parameter. The ~50 kHz splitting remained below the pure lipid T_c, reflecting the 'state of intermediate fluidity' or the presence of the now so-called liquid-ordered phase (lo). The ^{2}H n.m.r. technique was then developed rapidly by Seelig in Basel [11] using specifically deuterated lipids, and its progression still continues unabated (see [12–14] for reviews).

Two further useful developments in the ^{2}H n.m.r. area came from the works of Bloom, Davis and their colleagues [15, 16]. The first involved use of a spin-echo method [15], which permits the acquisition of relatively undistorted ^{2}H n.m.r. spectra, which would otherwise be distorted in a one-pulse technique as a consequence of pulse-feedthrough. The second involved

numerical methods to remove the broadening caused by the powder pattern distribution — the 'Pake doublet', dubbed 'de-Paking' by Bloom and colleagues ([16] and references therein). We have now added a second deconvolution method, the Levenburg–Marquart algorithm [17], in which de-Paked spectra are further deconvoluted to give individual resonances for each labelled site, and a typical result on a 1-[$^2H_{31}$]-palmitoyl-2[(9Z)octadec-9-enoyl]-*sn*-glycero-3-phosphocholine (palmitoyl oleoyl phophatidylcholine, POPC/cholesterol system (3:1 molar ratio, 1:1 wt ratio with H_2O) is shown in Fig. 2. The resolution is very good and we believe the method permits more accurate spectral analyses.

Using such well resolved spectra, we have investigated the condensing effects of a number of sterols other than cholesterol (H. Le & E. Oldfield, unpublished work) and have found that cholesterol is the most effective sterol in causing chain condensation. Addition of e.g. ring methyl groups causes decreased ordering compared with the effect of cholesterol, and could be explained by a tendency towards a surface 'ruffling' effect of the sterol nucleus. The results of an extensive series of studies in the late 1970s and early 1980s by our group, Bloom, Dahlquist, Seelig and others [18–22], led to a general picture of protein–lipid interaction in membranes in which there was little ordering of lipid acyl chains by protein. Rather, chain (and headgroup [22]) motions appear to slow down considerably in the presence of protein but, in general, the chains do not order in the way they do with cholesterol.

The ^2H n.m.r. method is not restricted to studies of hydrocarbon chain order and dynamics, as shown in early work by Seelig [23]. Unfortunately, it is not yet possible to unambiguously assign headgroup conformations for very flexible headgroups, like choline, on the basis of n.m.r. results alone. Much better progress has been made with glycolipids such as cerebroside since there are a number of fixed connectivities in the sugar group. With multiple-site labelling, good results for headgroup orientation can be obtained, both for cerebrosides [24] and many mono- and diglycosyldiglycerides [25]. A representative picture of cerebroside orientations in model membranes is given in Fig. 3, and analogous results have been obtained for the glycosylglycerolipids in elegant ^2H n.m.r. studies performed by Smith, Jarrell and their colleagues [25]. It seems plausible that this basic extended conformation applies to the galactosyl headgroups of cerebrosides in myelin, although this will be difficult to test experimentally.

^{13}C n.m.r. studies

So far, I have discussed results obtained for lipid, lipid/sterol and lipid/protein systems. The next step is, of course, to investigate what happens when all three components are mixed together and to try to see how the interactions in the model system compare with those seen in real biological

membranes. Proton n.m.r. spectra of even the lipid/sterol systems are of limited use because the sterol protons are, for the most part, 'invisible' under high-resolution MAS n.m.r. conditions. Deuterium n.m.r. is a good candidate — at least for model systems — and we have found in model DMPC/cholesterol/gramicidin systems, using ^2H-labelled lipids, that cholesterol dominates the ^2H quadrupole splitting (J. Patterson, T. Bowers & E. Oldfield, unpublished work), although the rates of motion appear to decrease. ^2H n.m.r. appears to be very useful for investigating the model-

Fig. 2. 55.7 MHz (8.45 Tesla) ^2H n.m.r. spectra of POPC/cholesterol (3:1 molar ratio, 50 wt% H_2O) at 37 °C

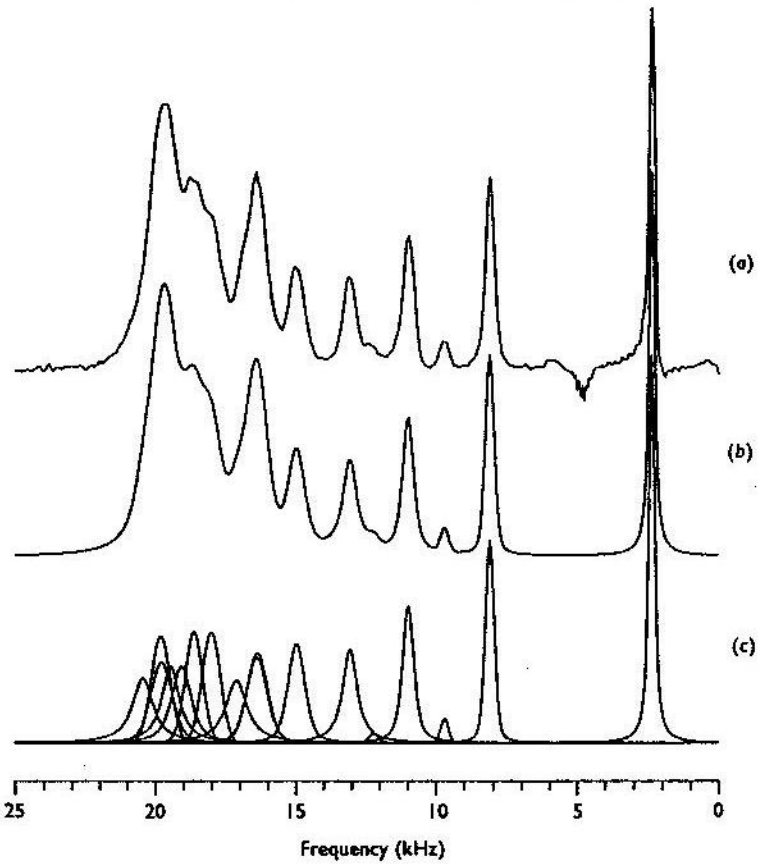

(a) De-Paked half spectrum; (b) deconvoluted (Levenburg–Marquardt) de-Paked half spectrum; (c) individual component lines in (b).

Fig. 3. Cerebroside headgroup orientations deduced from a conformational analysis of ^2H n.m.r. spectra of selectively deuterated *N*-hexadecanoylgluco-cerebroside (PGLC), at 90 °C

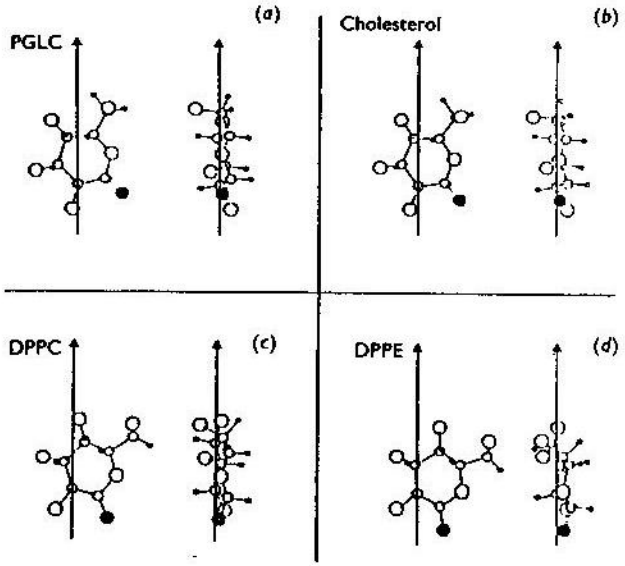

(a) PGLC; (b) 1:1 molar ratio PGLC/cholesterol; (c) 17 wt% PGLC in DPPC; (d) 17 wt% PGLC in dipalmitoylphosphatidylethanolamine. The arrows represent the bilayer normal, and the solid circles are the glycosidic oxygens. The structure on the right of each pair is generated by a 90° rotation of the left-hand structure about the bilayer normal. The hydroxymethyl group is shown to aid visualization of the ring, but the A_6 torsion angle is arbitrary. Reprinted from [24] with permission.

compound-containing systems, but is going to be of limited use in studies of many biomembranes, e.g. myelin and the red cell. However, as ourselves and others showed early on [26, 27] the technique can be used to investigate the structures of some biological membranes, i.e. those that can be biosynthetically enriched with ^2H-labelled fatty acids (or sterols).

What is required for more general studies of 'intact' biomembrane structure is a high resolution, natural abundance technique, and ^{13}C n.m.r. fits the bill.

Our earliest ^{13}C n.m.r. attempts [28, 29] on unsonicated multibilayers with and without cholesterol and on rat liver mitochondrial membranes, although of limited resolution and sensitivity, were nonetheless encouraging, and we asserted that 'studies on ^{13}C nuclei in higher fields, with lipids and membranes, where resolution is enhanced by an increased chemical shift range may be particularly useful' [2]. We were correct, but it took over a decade of developments in magnet technology to get to the point where these resolution (and sensitivity) improvements were actually achievable.

We show in Fig. 4 typical ^{13}C MAS n.m.r. results on lecithin and lecithin/cholesterol bilayers, together with conventional 'solution' ^{13}C n.m.r. results, without MAS, on sonicated bilayers [30]. For reasons that are well understood, the MAS n.m.r. technique gives remarkably better resolved ^{13}C spectra of the rigid sterol nucleus, which has led to the application of the technique to an analysis of an intact cell membrane, in this case the myelin membrane, from human brain [5]. Fig. 5 shows the 11.7 Tesla (500 MHz ^1H, 125 MHz ^{13}C) ^{13}C MAS n.m.r. spectrum of a sample of myelin taken from a neurologically normal adult, in which a large number of resonances can be resolved and assigned [5]. Such resolution is by far the best achieved to date on an intact biological membrane, the myelin membrane being a particularly attractive one for study because of its low water content, high lipid and sterol content, and the possible implications of any results obtained to human disease, an example being the contrast enhancement observed in MRI of abnormal and developing human myelins.

In ^{13}C n.m.r., the direct order-parameter information seen in ^2H n.m.r. is lost, but the trade-off is that many new systems which cannot be labelled, e.g. atherosclerotic plaque, lung surfactant, red cell membranes and myelin, become amenable to study. In addition, with ^{13}C n.m.r., there are qualitatively different types of spectroscopic parameters which can be used as structural probes, examples being the chemical shift [5], radiofrequency field-induced transverse relaxation (F. Adebodun, J. Chung, B. Montez, E. Oldfield & X. Shan, unpublished work), differential linebroadening [31, 32] and cross-relaxation. Figs. 6–9 give some idea of what might be in store. For example, we show in Fig. 6 ^{13}C MAS n.m.r. spectra of the natural plant glycolipid digalactosyldiglyceride (as a 1:1 wt ratio dispersion in H_2O) at 20, −10 and −30 °C. At 20 °C, essentially all carbons in the molecule are very well resolved, while at −30 °C, all of the headgroup, backbone carbons and the first two or three carbons of the acyl chain are broadened beyond detection. This can be explained by an interference effect between the coherent radiofrequency decoupling field and the incoherent thermal motions in the molecule and, as has been shown previously by others [33, 34], when the rate of motion of the C—H vector of interest is about the same as the radiofrequency field strength (in Hz), then decoupling is ineffective and considerable linebroadening ensues [32]. In DGDG, we see that the headgroup region is the first to become immobile (possibly coincidentally with bulk water freezing) on cooling, and that this effect is then transmitted along the acyl chains into the hydrocarbon interior. In our DGDG sample, 18:3 is the major fatty acid and, on cooling, it is possible to see, sequentially, Δ^9, Δ^{12} and then Δ^{15} 'freeze-out' or broaden. Such r.f. field-induced transverse relaxation could be a useful probe of lipid bilayer dynamics.

Fig. 4. **125 MHz (11.7 Tesla) proton-decoupled ^{13}C Fourier transform n.m.r. spectra at 21 °C of lecithin and lecithin/cholesterol (1:1) samples**

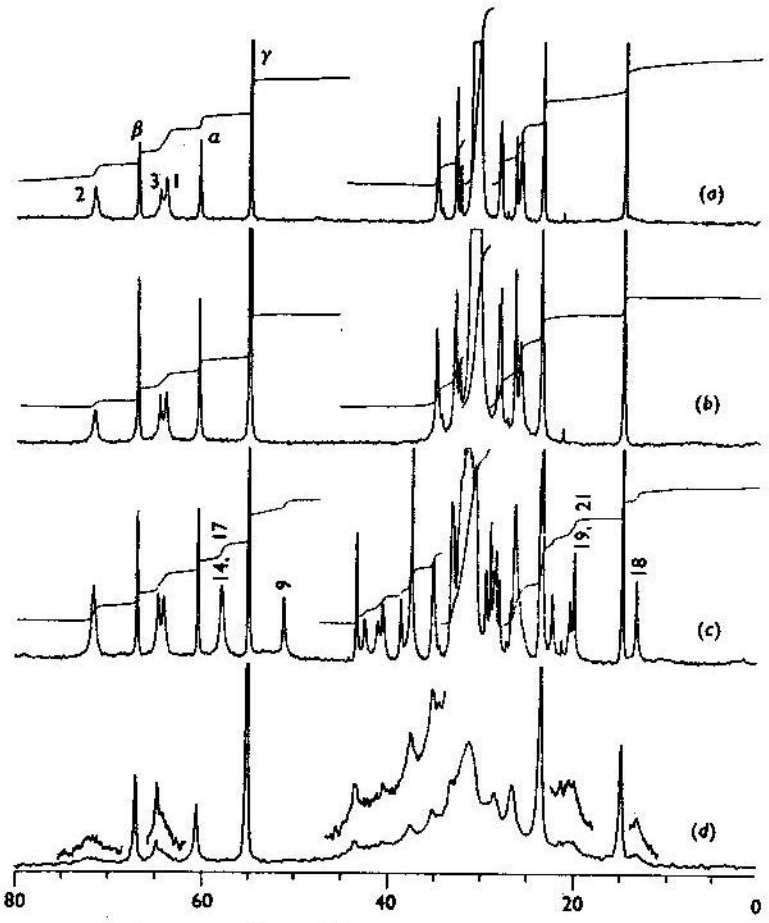

(a) Proton-decoupled ^{13}C MASS (2.1 kHz) n.m.r. spectrum of egg yolk lecithin (50 wt%)–D_2O at ~ 40-W continuous wave (CW) ^1H decoupling; (b) nuclear Overhauser effect enhanced, proton-decoupled ^{13}C n.m.r. spectrum of sonicated egg yolk lecithin (12.7 wt%)–D_2O at ~ 5-W WALTZ-16 ^1H decoupling; (c) proton-decoupled ^{13}C MASS (2.8 kHz) n.m.r. spectrum of egg yolk lecithin (33 wt%) cholesterol (17 wt%)–D_2O (50 wt%) at ~ 40-W CW ^1H decoupling; (d) nuclear Overhauser effect enhanced, proton-decoupled ^{13}C n.m.r. spectrum of sonicated egg yolk lecithin (8.5 wt%)–cholesterol (4.2 wt%)–D_2O (87.3 wt%) at ~ 5-W WALTZ-16 ^1H decoupling. An exponential line broadening of 6 Hz was applied to each spectrum. Recycle times of 5 s were used in all spectra shown. Reproduced from [30] with permission.

Fig. 5. **125.7 MHz (11.7 Tesla) proton-decoupled ^{13}C Fourier transform MAS n.m.r. spectrum of human adult myelin (43 years, male, myocardial infarct) at 37 °C**

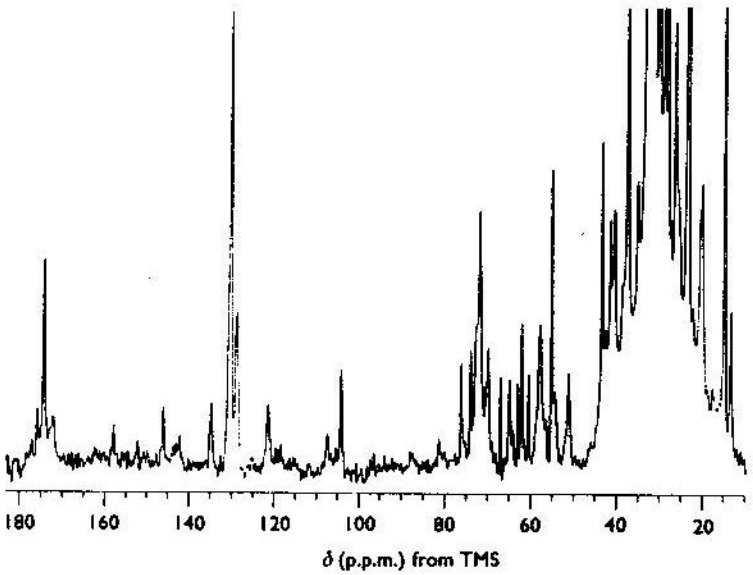

Spectral conditions are as follows: 3 kHz MAS rate, 16452 accumulations, 5 s recycle time, 2X 8k data points, ^{13}C 90° pulse width = 9 μs, 10 Hz linebroadening due to exponential multiplication.

A second interesting phenomenon that we have observed in liquid-crystalline phase bilayers, as well as in nematic and cholesteric liquid crystals and some polymers, is that of differential linebroadening of 'J-coupled' multiplets ([32] and references therein). An excellent example of this effect is shown in Fig. 7, where we are observing the proton-coupled ^{13}C MAS n.m.r. spectrum of the tricyclic antidepressant drug, desipramine, in a DMPC bilayer — a system previously investigated by Chapman, Cater and colleagues [35]. The differential linebroadening effect for the desipramine sp^2 carbons is thought to be caused by interference effects between the ^{13}C—^1H dipolar and the ^{13}C chemical shift anisotropy interactions, the result of which is that each component of the C—H doublet has a different relaxation rate, or linewidth. However, the effects are not equal for each of the four ring methine carbons: two have large differential linebroadening effects and two have much smaller ones, as may be seen in Fig. 7. The likely origin of these different linewidths is the motional averaging of the C—H dipolar interaction: two of the ring C—H vectors are approximately along the $C_{(2)}$

Fig. 6. **125.7 MHz (11.7 Tesla) proton-decoupled ^{13}C MAS n.m.r. spectra of a natural plant digalactosyldiglyceride, at the temperatures indicated**

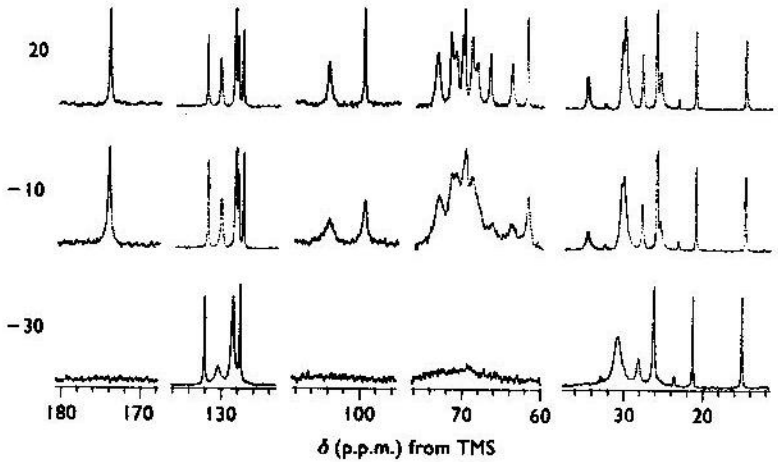

Spectral conditions are basically as described in Fig. 5.

axis of the molecule and two are close to the 'magic-angle' of 54.7°. Thus, fast rotation about the ring $C_{(2)}$ axis causes averaging of the dipolar interaction for C2 and C3 whereas the dipolar interactions at C1 and C4 are not appreciably averaged, and these sites have a large differential line-broadening. Similar effects are seen in other parts of the DMPC or DMPC/desipramine bilayer system and, certainly for model systems, coupled MAS n.m.r. spectra are likely to be a source of useful new information.

The third effect we wish to mention in our brief discussion of ^{13}C n.m.r. is that of cross-polarization (CP) [36]. The general technique of cross-polarization 'magic-angle' sample-spinning (CP-MAS) is by now probably well known, although we have not generally employed it in our membrane studies, as accurate estimates of peak intensities are difficult to achieve. The reason for this, however, is very interesting.

Now, in rigid solids, the rate at which ^{13}C magnetization increases in the CP experiment, for many protonated carbons, is fairly constant and of the order of several hundred microseconds. Membranes, on the other hand, have a wide range of rates and types of motion, and the rates at which magnetization builds up (and decays) vary over one or two orders of magnitude, as a result of the large range of motionally averaged dipolar interactions. A very typical result is seen in the two spectra shown in Fig. 8. In Fig. 8(*a*) we show a typical proton-decoupled Bloch decay spectrum of a

Fig. 7. **125.7 MHz (11.7 Tesla) proton-coupled ^{13}C MAS n.m.r. spectra of desipramine-1,2-ditetradecanoyl-*sn*-glycero-3-phosphocholine, 50 wt% water dispersion, at 40 °C**

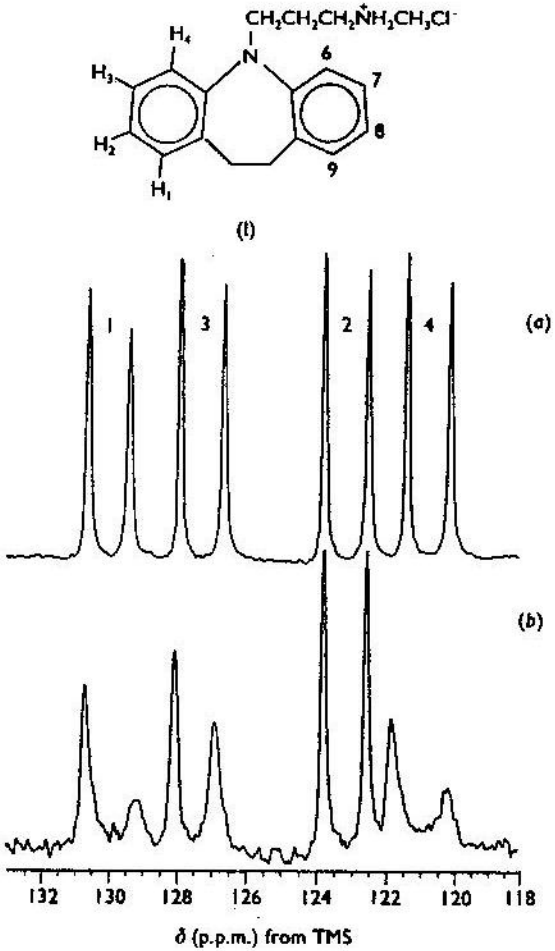

(a) 68.8 molar % desipramine (lipid basis); (b) 35.9 molar % desipramine; structure of desipramine shown above. Spectral conditions are basically as described in Fig. 5. The two broader doublets arise from C—H vectors (C1—^{1}H, C4—^{1}H) aligned approximately along the $C_{(2)}$ axis of desipramine, while the narrower doublets are thought to arise from C—H vectors aligned closer to the 'magic-angle' (C2—^{1}H, C3—^{1}H), result mix-time. With spectral editing, all mobile headgroup carbons, galactose C1–6, duced from [32] with permission.

Fig. 8. **125.7 MHz (11.7 Tesla) ^{13}C MAS n.m.r. spectra of 1,2-ditetradecanoyl-*sn*-glycero-3-phosphocholine, 50 wt% H_2O, at 37 °C**

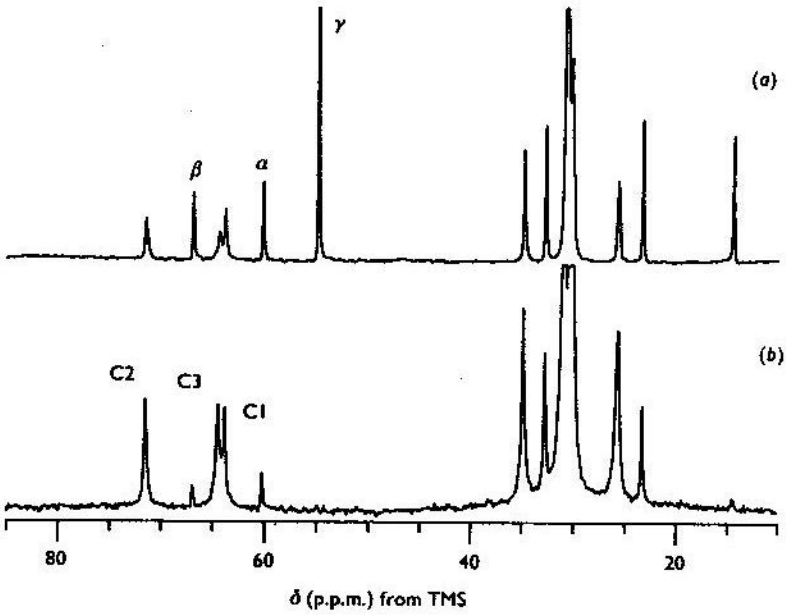

(a) Proton-decoupled Bloch decay spectrum showing approximately equal intensities for all types of carbon; (b) CP spectrum obtained using a 300 μs mix-time, showing spectral selection of rigid backbone and acyl side-chain carbons.

sample of DMPC, in excess water (50 wt% H_2O), at 37 °C. All peaks have close to the theoretical intensity on the basis of structural considerations. However, in a CP spectrum at short mix times, which accentuates the more rigid, dipolar-coupled spin signal intensities, a very different result is obtained (Fig. 8*b*) in which there is strong spectral editing in favour of the more rigid sites, there being little intensity from e.g. the mobile choline or terminal methyl groups. Thus, spectra can be edited on the basis of their 'solidity', or T_{CH}^{-1} cross-relaxation rate constants.

We believe this spectral-editing technique may have considerable use in simplifying complex biomembrane spectra. By way of example, we show in Fig. 9 the conventional ^1H-decoupled Bloch decay spectrum of a sample of human myelin (Fig. 9*a*) together with, for comparison, a spectrally edited myelin spectrum obtained using a 30 ms CP mix-time (Fig. 9*b*) which selects for the mobile groups (as opposed to the solid selection shown in Fig. 8*b*). Clearly, a remarkable simplification results from editing and, in the edited

Fig. 9. **125.7 MHz (11.7 Tesla) ^{13}C MAS n.m.r. spectra of human adult myelin, showing spectral selection of mobile headgroup carbon atom sites**

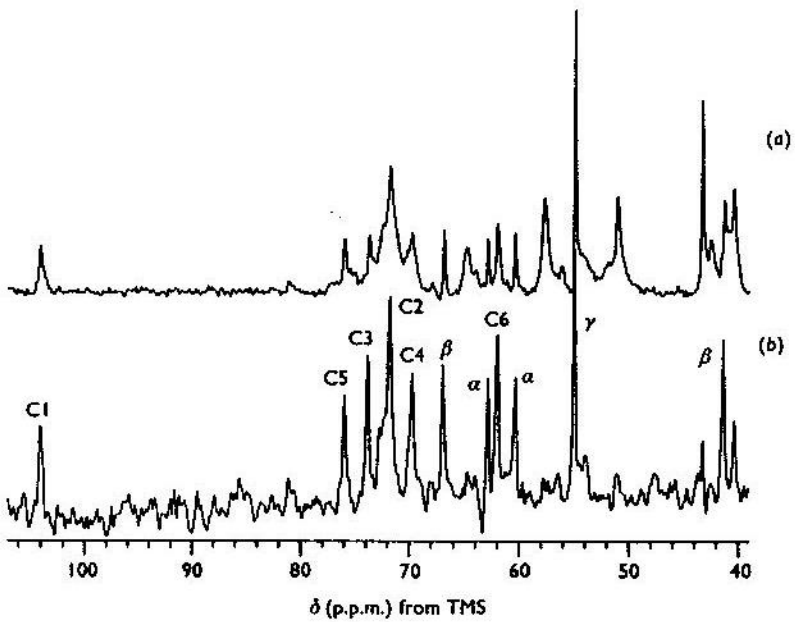

(a) Proton-decoupled Bloch decay spectrum; (b) CP spectrum obtained using a 30 ms mix-time. With spectral editing, all mobile headgroup carbons, galactose C1–6, PC/SM C^{α}, C^{β}, C^{γ}, and PE/PE-plasmalogen $C^{\alpha,\beta}$, can be resolved, demonstrating the high mobility of a major fraction of the myelin membrane headgroup sugar and phospholipid sites.

spectrum, all of the expected headgroup carbons, C1–6 of cerebroside, C^{α}, C^{β} and C^{γ} of phosphatidylcholine (PC)/sphingomyelin (SM) and C^{α} and C^{β} of phosphatidylethanolamine (PE) can be assigned — including the otherwise very difficult to resolve PE C^{β} and galactose $C_{(2,4)}$ carbons. The fact that many of the galactose, PC/SM and PE carbons are quite intense at long mix times indicates clearly that many of the myelin headgroups are highly mobile, the rigid carbons being edited on the basis of their short T_{CH} and ^1H-rotating frame relaxation times.

Conclusions

We have attempted to give a brief overview of the developments which have occurred over the past 25 years in the study of membrane structure by n.m.r.

spectroscopy — the original experiments being carried out in the mid to late 1960s by Dennis Chapman and his colleagues.

Perhaps not surprisingly, many of the systems currently under investigation remain the same as those of 25 years ago, examples being lecithin, lecithin/cholesterol and myelin. Lecithin was chosen in the early days because it gave at least one sharp peak, from the choline NMe_3 group, and myelin was chosen because of its high lipid content. Fortunately, things have now progressed to the point where, by using either ^2H spin-echo/de-Paking/deconvolution, or ^{13}C MAS n.m.r. (coupled MAS, CP MAS, decoupled MAS), essentially every atomic site in lecithin, lecithin/cholesterol — or any other model lipid system and, to some extent, intact biomembranes — can be probed by means of solid-state n.m.r. spectroscopy. A much better understanding of protein–lipid interaction has been obtained, and now a number of researchers are using ^2H and ^{13}C n.m.r. to investigate peptides and membrane proteins themselves [37–41]. The general topics of lipid–sterol (and possibly lipid–sterol–protein) interaction are even beginning to have some impact in areas such as brain (myelin) development and disease, as a consequence of the interactions that occur between brain H_2O (observed in MRI) and the membrane lipids. It will be interesting to see what happens in the next 25 years.

This work was supported by the United States Public Health Service (grant GM-40426).

References

1. Chapman, D. & Penkett, S. A. (1966) Nature (London) 211, 1304–1305
2. Chapman, D., Oldfield, E., Doskočilová, D. & Schneider, B. (1972) FEBS Lett. 25, 261–264
3. Lawson, K. D. & Flautt, T. J. (1968) J. Phys. Chem. 72, 2066–2074
4. Forbes, J., Husted, C. & Oldfield, E. (1988) J. Am. Chem. Soc. 110, 1059–1065
5. Forbes, J., Bowers, J., Moran, L., Shan, X., Oldfield, E. & Moscarello, M. A. (1988) J. Chem. Soc., Faraday Transactions 84, 3821–3849
6. Wennerström, H. (1973) Chem. Phys. Lett. 18, 41–44
7. Koenig, S. H., Brown III, R. D., Spiller, M. & Lundbom, N. (1990) Mag. Res. Med. 14, 482–495
8. Fralix, T. A., Ceckler, T. L., Wolff, S. D., Simon, S. A. & Balaban, R. S. (1991) Mag. Res. Med. 18, 214–223
9. Vist, M. R. & Davis, J. H. (1990) Biochemistry 29, 451–464
10. Oldfield, E., Chapman, D. & Derbyshire, W. (1971) FEBS Lett. 16, 102–104
11. Seelig, J. (1977) Quart. Rev. Biophys. 10, 353–418
12. Smith, R. L. & Oldfield, E. (1984) Science 225, 280–287
13. Davis, J. H. (1989) Adv. Magn. Res. 13, 195–223
14. Griffin, R. G. (1981) Methods Enzymol. 72, 108–174
15. Davis, J. H., Jeffrey, K. R., Bloom, M., Valic, M. I. & Higgs, T. P. (1976) Chem. Phys. Lett. 42, 390–394
16. Whittall, K. P., Sternin, E., Bloom, M. & MacKay, A. L. (1989) J. Magn. Res. 84, 64–71
17. Press, W. H., Flannery, B. P., Teukolsky, S. A. & Vetterling, W. T. (1986) in Numerical Recipes: the Art of Scientific Computing, pp. 523–528, Cambridge University Press, New York
18. Kang, S. Y., Gutowsky, H. S., Hsung, J. C., Jacobs, R., King, T. E., Rice, D. & Oldfield, E. (1979) Biochemistry 18, 3257–3267
19. Paddy, M. R., Dahlquist, F. W., Davis, J. H. & Bloom, M. (1981) Biochemistry 20, 3152–3162
20. Seelig, A. & Seelig, J. (1978) Hoppe-Seyler's Z. Physiol. Chemie 359, 1747–1756
21. Meier, P., Sachse, J. H., Brophy, P. J., Marsh, D. & Kothe, G. (1987) Proc. Natl. Acad. Sci. U.S.A. 84, 3704–3708

22. Rajan, S., Kang, S. Y., Gutowsky, H. S. & Oldfield, E. (1981) J. Biol. Chem. 256, 1160–1166
23. Seelig, J., Gally, H.-U. & Wohlgemuth, R. (1977) Biochim. Biophys. Acta 467, 109–119
24. Skarjune, R. & Oldfield, E. (1982) Biochemistry 21, 3154–3160
25. Jarrell, H. C., Jovall, P. Å., Giziewicz, J. B., Turner, L. A. & Smith, I. C. P. (1987) Biochemistry 26, 1805–1811
26. Oldfield, E., Chapman, D. & Derbyshire, W. (1972) Chem. Phys. Lipids 9, 69–81
27. Stockton, G. W., Johnson, K. G., Butler, K. W., Tulloch, A. P., Boulanger, Y., Smith, I. C. P., Davis, J. H. & Bloom, M. (1977) Nature (London) 269, 267–268
28. Oldfield, E. & Chapman, D. (1971) Biochem. Biophys. Res. Commun. 43, 610–616
29. Keough, K. M., Oldfield, E., Chapman, D. & Beynon, P. (1973) Chem. Phys. Lipids 10, 37–50
30. Oldfield, E., Bowers, J. L. & Forbes, J. (1987) Biochemistry 26, 6919–6923
31. Oldfield, E., Chung, J., Le, H., Bowers, T., Patterson, J. & Turner, G. L. (1992) Macromolecules 25, 3027–3030
32. Adebodun, F., Chung, J., Montez, B., Oldfield, E. & Shan, X. (1992) Biochemistry 31, 4502–4509
33. Rothwell, W. P. & Waugh, J. S. (1981) J. Chem. Phys. 74, 2721–2732
34. VanderHart, D. L., Earl, W. L. & Garroway, A. N. (1981) J. Magn. Res. 44, 361–401
35. Cater, B. R., Chapman, D., Hawes, S. M. & Saville, J. (1974) Biochim. Biophys. Acta 363, 54–69
36. Pines, A., Gibby, M. G. & Waugh, J. S. (1972) J. Chem. Phys. 56, 1776–1777
37. Nicholson, L. K., Moll, F., Mixon, T. E., LoGrasso, P. V., Lay, J. C. & Cross, T. A. (1987) Biochemistry 26, 6621–6626
38. Creuzet, F., McDermott, A., Gebhard, R., van der Hoef, K., Spijker-Assink, M. B., Herzfeld, J., Lugtenburg, J., Levitt, M. H. & Griffin, R. G. (1991) Science 251, 783–786
39. Prosser, R. S., Davis, J. H., Dahlquist, F. W. & Lindorfer, M. A. (1991) Biochemistry 30, 4687–4696
40. Cornell, B. A., Separovic, F., Baldassi, A. J. & Smith, R. (1988) Biophys. J. 53, 67–76
41. Bowers, J. L. & Oldfield, E. (1988) Biochemistry 27, 5156–5161